Valence quark contribution for the $\gamma N \to \Delta$ quadrupole transition extracted from lattice QCD

G. Ramalho[1,2] and M. T. Peña[2,3]

[1]*Thomas Jefferson National Accelerator Facility, Newport News, Virginia 23606, USA*
[2]*Centro de Física Teórica de Partículas, Avenida Rovisco Pais, 1049-001 Lisboa, Portugal*
[3]*Department of Physics, Instituto Superior Técnico, Avenida Rovisco Pais, 1049-001 Lisboa, Portugal*

(Received 27 January 2009; published 16 July 2009)

Starting with a covariant spectator quark model developed for the nucleon N and the Δ in the physical pion mass region, we extend the predictions of the reaction $\gamma N \to \Delta$ to the lattice QCD regime. The quark model includes S and D waves in the quark-diquark wave functions. Within this framework, it is the D-wave part in the Δ wave function that generates nonzero valence contributions for the quadrupole form factors of the transition. Those contributions are however insufficient to explain the physical data, since the pion cloud contributions dominate. To separate the two effects, we apply the model to the lattice regime in a region where the pion cloud effects are negligible and adjust the D-state parameters directly to the lattice data. This process allows us to obtain a better determination of the D-state contributions. Finally, by adding a simple parametrization of the pion cloud, we establish the connection between the experimental data and the lattice data.

DOI: 10.1103/PhysRevD.80.013008 PACS numbers: 13.40.Gp, 12.38.Gc, 12.39.Ki

I. INTRODUCTION

In recent years, the structure of the baryon resonances has been an important topic of both experimental and theoretical investigation. Of particular interest is the Δ resonance, the first excited state of the nucleon. New Δ photo-production data for large four-momentum transfer have been extracted in several laboratories, as Jlab, MAMI, LEGS, and MIT-Bates [1–5]. Simultaneously, lattice simulations were performed for both the $\gamma\Delta \to \Delta$ [6,7] and the $\gamma N \to \Delta$ [8–10] transition form factors.

This last transition can be described in terms of the Jones and Scadron multipole form factors [11]: the magnetic dipole M1 (G_M^*), the electric E2 (G_E^*), and the Coulomb C2 (G_C^*) quadrupole form factors. The reaction is dominated by the magnetic dipole form factor G_M^*. Although constituent quark models [12–20], with valence quark degrees of freedom only, are sufficient to explain some properties of the Δ, they are not sufficient to explain the G_M^* data at the physical point ($m_\pi = m_\pi^{phy} = 138$ MeV) [12,13,21]. The inclusion of chiral symmetry and/or a coupling of the quark to the pion field [22–25] helps to overcome the limitations of the pure valence quark models. The importance of the pion field, or ''pion cloud,'' was also demonstrated using effective field theory [26–28] and model reaction mechanisms based on the hadronic fields, known as dynamical models [29–31]. See Ref. [21] for a review of the $\gamma N \to \Delta$ transition.

In previous works we successfully described the nucleon [32,33], the $\gamma\Delta \to \Delta$ [34], and the $\gamma N \to \Delta$ [12,13] transitions, by considering a spectator quark model inspired by the vector meson dominance (VMD) mechanism. When we restrict the Δ wave function to S waves, the spectator valence quark model gives no contributions to the quadrupole form factors G_E^* and G_C^* [12]. Those contributions emerge only when D states are considered, consistent with other constituent quark models [14,15]. The D states improve the description of the experimental data, but their contributions are in general small, with the quadrupole form factors at the physical point being dominated by the pion cloud [13] (see also [16,21] for a review). The dominance of the pion cloud at the physical point prevents an accurate calibration of the valence quark D-state contributions and, consequently, the relative amount of the contributions from D waves only and the pion cloud is not yet exactly known [13,21,30].

The VMD mechanism, which we used to parametrize the electromagnetic interaction in terms of the hadronic masses, can also be used to extend the covariant spectator model to the lattice regime. By introducing the dependence of the hadronic masses on the lattice pion mass, we could describe the lattice data for the nucleon [35] and for the magnetic dipole form factor G_M^* [10] of the $\gamma N \to \Delta$ reaction, with only S waves in both the nucleon and the Δ wave functions [36]. This motivated us to include D states in the Δ wave function in the present work to show whether the description of the lattice data is still possible, also for the G_E^* and G_C^* form factors.

In order to include the D states, and to overcome the uncertainty discussed above on their effects, we start by realizing that the valence quark effects are expected to dominate for large pion masses, exactly when pion cloud effects are expected to be suppressed [37]. In light of this, lattice QCD, in particular, in quenched approximation with $m_\pi > 400$ MeV (where the pion cloud effects are negligible [37]) becomes the ideal laboratory to test the valence quark contributions and to constrain the D states. Importantly, the dependence of the two subleading G_E^* and G_C^* form factors on the D states allows then the extraction of very relevant information.

In this work we use the lattice information to determine more precisely the valence quark effects in the $\gamma N \to \Delta$ quadrupole form factors, and we consider the contributions of the valence quark structure, including orbital D states, in the regime of the lattice calculations. First, we started by making a direct application of the valence quark model fixed in the physical region ($m_\pi = m_\pi^{\rm phy}$) in Ref. [13], to the quadrupole moments in the lattice region. Although the model generates the correct order of magnitude of the lattice quadrupole data, it fails to reproduce their Q^2 dependence. Therefore, we inverted the procedure: we began by readjusting the Δ model parametrization to the quenched lattice data, imposing an overall description of the lattice data for several values of the pion mass. From the resulting parametrization, we generated directly the valence quark contribution of the orbital D states to G_E^* and G_C^* at the physical point. Finally, by adding a pion cloud contribution derived in the large-N_c limit, which was established independently from our model, we obtain a successful description of the experimental data.

The paper is organized as follows: in Sec. II we review the formalism associated with the spectator quark model; in Sec. III we explain how to generalize the model to the lattice QCD regime; in Sec. IV we present the results of that generalization; in Sec. V we present the predictions for the quadrupole form factors in the physical region and discuss the results; finally, in Sec. VI we draw conclusions.

II. FORMALISM

We consider a quark model based on the covariant spectator formalism [38,39]. In this formalism, the nucleon and the Δ are described as a system of an off-mass-shell quark and two noninteracting quarks forming an on-mass-shell diquark [12,13,32,39].

In our model, the quarks are effective degrees of freedom ''dressed'' by form factors, and the nucleon and Δ wave functions are not derived from a dynamical wave equation, but given a parametric form consistent with the intrinsic symmetries of these systems. By construction , the wave functions are covariant and reproduce their expected nonrelativistic limits. The first feature is important for the application of the formalism to the kinematics of the recent data.

The nucleon and Δ wave function can be expressed in terms of a quark spin (isospin) state together with a spin-0 (isospin-0) diquark state and a spin-1 (isospin-1) vector diquark state [12,32,33], multiplied by a relative angular momentum state [13].

The electromagnetic transition current between the nucleon and the Δ can be expressed [12,13,32,33] as

$$J^\mu = 3\sum_\lambda \int_k \bar{\Psi}_\Delta(P_+, k) j_I^\mu \Psi_N(P_-, k), \tag{1}$$

where j_I^μ is a generic isospin dependent quark current, Ψ_Δ, Ψ_N are, respectively, the wave function of the nucleon (momentum P_-) and Δ (momentum P_+). The hadronic current (1) involves the sum in all intermediate diquark polarizations $\lambda = 0, \pm 1$, and the invariant integral $\int_k \equiv \int \frac{d^3k}{2E_s(2\pi)^3}$ over the diquark momentum, where E_s is the diquark on-mass-shell energy $E_s = \sqrt{m_s^2 + \mathbf{k}^2}$ (m_s is the diquark mass). The factor 3 accounts for the flavor symmetry.

For the quark current, we consider the general form

$$j_I^\mu = j_1 \gamma^\mu + j_2 \frac{i\sigma^{\mu\nu} q_\nu}{2m_N}, \tag{2}$$

where m_N is the nucleon mass and j_1, j_2 contain the quark form factors, which depend on the transferred four-momentum squared Q^2. They can be decomposed into isoscalar (+) and isovector (−) operators that act in the baryon isospin states according to

$$j_i(Q^2) = \tfrac{1}{6} f_{i+}(Q^2) + \tfrac{1}{2} f_{i-}(Q^2)\tau_3. \tag{3}$$

To represent the electromagnetic quark form factors $f_{i\pm}$ ($i = 1, 2$), we consider a parametrization inspired by VMD. In particular, following [12,13,32] we used

$$f_{1\pm}(Q^2) = \lambda + (1-\lambda)\frac{m_v^2}{m_v^2 + Q^2} + c_\pm \frac{Q^2 M_h^2}{(M_h^2 + Q^2)^2}, \tag{4}$$

$$f_{2\pm}(Q^2) = \kappa_\pm \left\{ d_\pm \frac{m_v^2}{m_v^2 + Q^2} + (1 - d_\pm)\frac{Q^2}{M_h^2 + Q^2} \right\}. \tag{5}$$

In this parametrization, λ was adjusted to give the charge number density in the deep inelastic limit [32]; m_v represents a vector meson ($m_v = m_\rho, m_\omega$), M_h is a mass of an effective heavy vector meson simulating the short-range structure, and κ_+ (κ_-) the isoscalar (isovector) quark anomalous moments. These two last values were adjusted to reproduce the nucleon magnetic moment $\kappa_+ = 1.639$ and $\kappa_- = 1.823$ [32]. The coefficients $c_\pm$ and $d_\pm$ were adjusted to reproduce the nucleon electromagnetic form factors. In the calculation presented here, we took the current parametrization corresponding to model II in Ref. [32] for the nucleon elastic form factors. The explicit values of the VMD coefficients are $c_+ = 4.16$, $c_- = 1.16$, and $d_\pm = -0.686$. For the effective heavy meson, we took $M_h = 2m_N$. The values for λ and the diquark mass are 1.21 and $m_s = 0.87\ m_N = 817$ MeV, respectively.

For both the nucleon and the Δ, we consider wave functions that contain the correct spin-isospin structure, with orbital parts modeled by scalar functions ϕ of the quark four-momentum squared $(P-k)^2$, expressed in terms of the ratio

$$\chi_H = \frac{(m_H - m_s)^2 - (P-k)^2}{m_H m_s}, \tag{6}$$

where m_H represents the nucleon or the Δ mass (m_N and m_Δ).

For the nucleon, we consider an S-state wave function [12,32,33], including a mixture of a spin 0 and isospin 0 with a spin-1 and isospin-1 diquark structure. In particular we used

$$\phi_N(P,k) = \frac{N_0}{m_s(\beta_1 + \chi_N)(\beta_2 + \chi_N)}, \tag{7}$$

where N_0 is a normalization constant. The parameters β_1 and β_2 ($\beta_2 > \beta_1$) can be interpreted as Yukawa mass parameters. Then β_2 accounts for the short-range physics and β_1 for the long range. The corresponding parameters can be found in Refs. [12,13,32].

As for the Δ, we consider an admixture of S and D states, where, as explained in Ref. [13], the D-state wave function decomposes into a spin $1/2$ core ($D1$ state) and a spin $3/2$ core ($D3$ state), both with isospin $3/2$:

$$\Psi_\Delta = N[\Psi_S + a\Psi_{D3} + b\Psi_{D1}], \tag{8}$$

where a and b are admixture coefficients, Ψ_S represents the (symmetric) Δ S state, and the remaining two possible D states. The normalization constant becomes $N = 1/\sqrt{1 + a^2 + b^2}$.

To represent the momentum probability distribution of the quark-diquark Δ system we have, as in [13],

$$\phi_S = \frac{N_S}{m_s(\alpha_1 + \chi_\Delta)^3}, \tag{9}$$

$$\phi_{D3} = \frac{N_{D3}}{m_s^3(\alpha_2 + \chi_\Delta)^4}, \tag{10}$$

$$\phi_{D1} = \frac{N_{D1}}{m_s^3}\left\{\frac{1}{(\alpha_3 + \chi_\Delta)^4} - \frac{\lambda_{D1}}{(\alpha_4 + \chi_\Delta)^4}\right\}. \tag{11}$$

Similar to the nucleon case, α_i are momentum range parameters, and N_X are normalization constants. Since, with the inclusion of the D states, the S state can be parametrized with only one range parameter (α_1), as shown in Ref. [13], we relabeled all the range parameters, with α_1 standing for the average of the values of the best model of Ref. [13]. In expression (11), the coefficient λ_{D1} was chosen to impose the orthogonality between the nucleon S state and the Δ $D1$ state (see Ref. [13] for details). The extra power in Eq. (9) when compared to the corresponding equation for the nucleon Eq. (7), was introduced to take into account the G_M^* falloff observed at low and intermediate Q^2 [12,13,21]. The dependence of the D states on the ratio χ_Δ was chosen to reproduce the behavior of the $\gamma N \to \Delta$ transition [13] in perturbative QCD.

All wave functions are normalized in order to reproduce the nucleon [12,32] and Δ [12,13,34] charge. In particular, one has [13]

$$\int_k [\phi_N(\bar{P},k)]^2 = \int_k [\phi_S(\bar{P},k)]^2 = 1, \tag{12}$$

$$\int_k [\tilde{k}^2\phi_{D3}(\bar{P},k)]^2 = \int_k [\tilde{k}^2\phi_{D1}(\bar{P},k)]^2 = 1, \tag{13}$$

where $\bar{P}$ represents the momentum in the respective baryon frame $\bar{P} = (m_H, 0, 0, 0)$. The variable $\tilde{k}$, defined as $\tilde{k} = k - \frac{P\cdot k}{m_H^2}P$, was introduced in Ref. [13] to represent the D states.

In summary, the nucleon (S state) wave function contains two range parameters (β_1 and β_2), the Δ S-state wave function contains a single parameter (α_1), and the Δ D states contain three (α_i, with $i = 2, 3, 4$) parameters. The D-state admixture is controlled additionally by the a and b parameters defined in Eq. (8). All of the parameters associated to the quark current and the nucleon wave function were fixed by the nucleon elastic data at the physical point in a previous work [32]. They are kept unchanged here, where we fit only five parameters to the lattice QCD data: the three range parameters and the two admixture coefficients for the two D states.

III. EXTENSION OF THE SPECTATOR MODEL TO THE LATTICE REGIME

Now we consider the extension of the model presented in the previous section, and based on the valence quark degrees of freedom, to the lattice QCD data region. As the pion cloud effects are expected to be suppressed for $m_\pi > 400$ MeV [37], it is justified in this region to consider the valence contributions only. Therefore, we generalize the original (valence) spectator model by considering the implicit dependence of all of the mass parameters on the pion mass. Since the wave functions depend on the ratio defined in Eq. (6), the diquark mass scales out from the current and consequently from the form factors [32]. The dependence of the model on the pion mass appears through both the quark current and the baryon wave functions. The quark form factors (4) and (5) in the current operator (2) are written in terms of a VMD parametrization, and therefore depend on a vector meson mass m_v and an effective heavy meson mass $M_h = 2m_N$. The extension to lattice is done by considering the nucleon and ρ masses from the lattice calculation as an implicit function of m_π.

The nucleon and Δ wave functions (7) and (9)–(11) are represented in terms of the (adimensional) momentum range parameters (β_i and α_i) and the kinematic ratio χ_H of Eq. (6). Because the mass dependence of the wave function enters in this ratio, we expect only a weak dependence on the range parameters (α_i and β_i) near the physical region. In fact, this weak sensitivity of the range parameters to the pion mass was already verified in the work of Ref. [36] for light pions. For this reason, we use the same range parameters both in the lattice data region and at the physical point, neglecting any pion mass dependence of

the range parameters in the considered region ($m_\pi <$ 600 MeV). For heavier pions, the interaction becomes almost pointlike, and at least the short-range coefficients should be corrected, or an explicit dependence on the pion mass introduced.

The procedure presented here corresponds to the case of Ref. [36] with $M_\chi = +\infty$ (M_χ is the constituent quark mass in the chiral limit). A more detailed treatment is possible with finite values of M_χ, but for the quadrupole lattice data, the corrections are small when compared to the statistical errorbands and the differences between the data sets associated with different values for the pion masses.

To start, we took the best valence quark model presented in Ref. [13], fixed for the physical data case ($m_\pi = m_\pi^{\rm phy}$). The analytical expressions for G_M^*, G_E^*, and G_C^* are presented in Ref. [13]. No readjustment of the parameters of the quark current and of the nucleon and Δ wave functions was made, except for the nucleon, Δ, and ρ masses, which are explicit functions of m_π, as in the lattice calculations. The mass parameters are presented in Table I.

Figure 1 shows the results of model 4 of Ref. [13] extended to the quenched lattice QCD calculations of Ref. [10]. We only show G_E^* and G_C^*, since G_M^* does not change much from [36]. The conclusion is that we cannot reproduce the lattice data accurately, but the predictions of the model have the right order of magnitude. The poor description of G_E^* and G_C^*, obtained from taking the physical model to the lattice domain, contrasts with what happens for the dominant G_M^* form factor obtained in Ref. [36]. It shows that the lattice data is more sensitive to the D-wave components of the Δ wave function—crucial for the quadrupole form factors—than to the S-wave components that dominate G_M^*. This makes the lattice data for the quadrupole form factors extremely interesting, as a potential source of information on the D-wave effects in the hadronic structure, and thus indirectly, on the magnitude of the pion cloud effects. In Ref. [13], when the model was applied to the physical point, the valence quark contributions were not explicitly separated from the pion cloud contributions. For that reason, the estimate of the valence contribution could not be made very precise, as we confirm in this extension to the lattice regime.

TABLE I. Masses in GeV, considered in lattice QCD [10] and at the physical point.

m_π	m_N	m_Δ	m_ρ
0.563	1.267	1.470	0.898
0.490	1.190	1.425	0.835
0 411	1.109	1.382	0.848
0.138	0.939	1.232	0.776

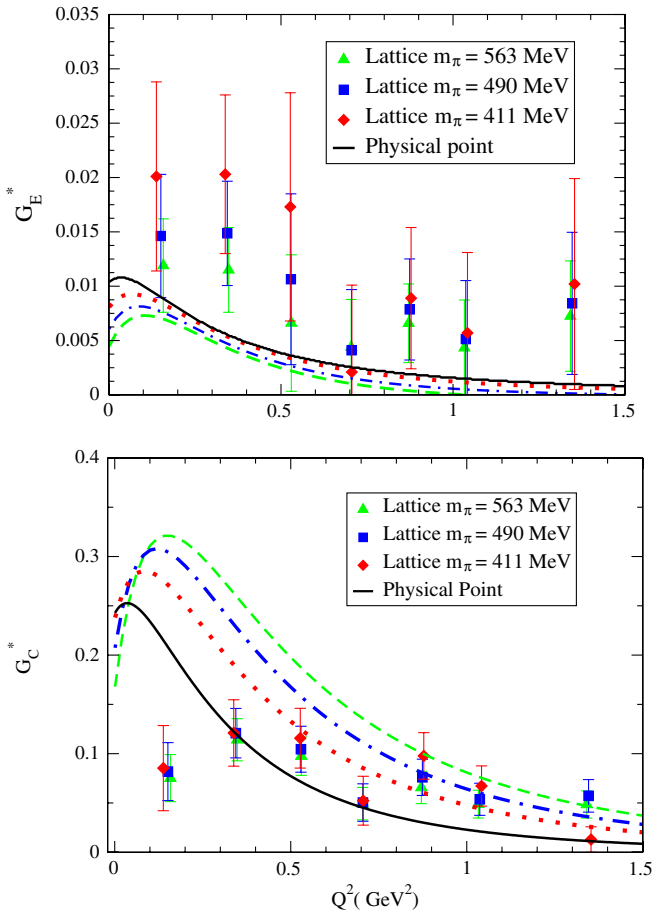

FIG. 1 (color online). Quadrupole form factors in quenched lattice QCD [10]. The lines correspond to the parametrization of the model 4 from Ref. [13]. The lattice data corresponds to $m_\pi = 563$ MeV (dashed line), 490 MeV (dot-dashed line), and 411 MeV (dotted line). The solid line is the valence quark contribution in the physical point (same result as in Ref. [13]).

IV. ADJUSTMENT OF THE D-STATE PARAMETERS TO THE LATTICE DATA

Given the results of the last section, we decided to change our strategy in the process of comparing the quark model results with the lattice data. Instead of trying to use the quadrupole data in the physical region, where valence and pion cloud contributions are both important, we fit first the lattice data and extrapolate to the physical point. With this procedure, we avoid ambiguities related to the exact contribution of the pion cloud mechanisms and their entanglement with the D-wave effects. The parameters which are varied in the fit are the admixture coefficients a and b and the three range parameters α_i ($i = 2, 3, 4$), all associated to the D-state scalar wave functions. We fit these five parameters to the lattice data. The S-state parameter (α_1) was not fitted, and the value $\alpha_1 = 0.3366$ from Ref. [13] was used.

The partial and total results for the χ^2 obtained are presented in Table II. The final results for the observables

TABLE II. Quality of the quenched fit in χ^2 (partial and total) for the three form factors at the respective pion mass. Quenched lattice QCD data from Ref. [10].

m_π (GeV)	$\chi^2(G_M^*)$	$\chi^2(G_E^*)$	$\chi^2(G_C^*)$	χ^2
0.563	0.569	0.483	0.853	0.618
0.490	0.544	0.290	0.668	0.513
0.411	1.956	0.548	1.163	1.406
Total				0.842

are presented in Figs. 2 and 3. The D-wave model parameters associated with the fit are presented in Table III.

The obtained range parameters are larger than the ones from the fit to the physical data [13], suggesting that the D states are less peripheral (i.e., have a shorter range in configuration space) than inferred in Ref. [13], where we used an indirect estimate of the valence quark contribution at the physical pion mass point, based on specific assumptions about the pion cloud contribution. Another interesting point is that the D-state range parameters $\alpha_i = 0.338 - 0.351$, with $i = 2, \ldots, 4$, do not spread over a large region, suggesting one single value, $\alpha_i \simeq 0.344$, as the signature range of the D-state regime, slightly larger than that of the S-state range $\alpha_1 \simeq 0.337$. We note that, in this case, it is the additional power in the D-state scalar wave functions [see Eqs. (9)–(11)] that implies a more peripheral character for those states, when compared with the S states. Indeed, as for low k, $\chi = \frac{k^2}{m_s^2}$ [39], a higher power in momentum space corresponds to a more peripheral effect in configuration space, as it is to be expected from a D-wave contribution. The best fit corresponds to an admixture of 0.72% for both $D3$ and $D1$ states in the Δ wave function.

Compared to the results obtained by using the physical data alone, the significant change occurs for the percentage of the $D1$ component, that drops from 4.36% to 0.72%. As for the state $D3$, the differences are minor. In Ref. [13] the percentage was 0.88%. As $a \simeq b$, we conclude that the quenched lattice data is consistent with an equal admixture for both D states. The initial number of effective parameters needed for a good fit can be reduced from five to four.

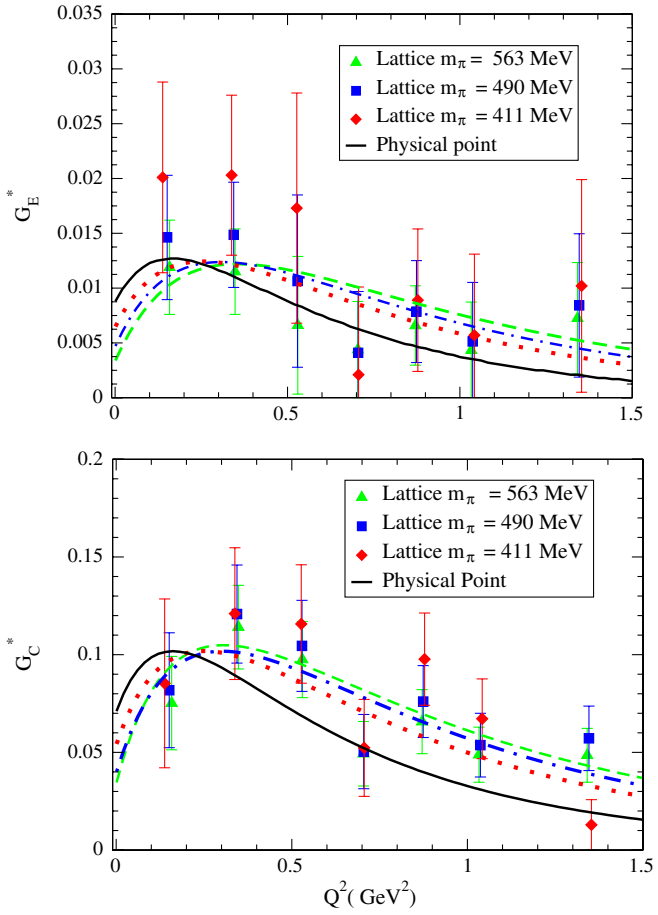

FIG. 3 (color online). Best fit of the quadrupole form factors in quenched lattice QCD [10]. The lines have the same meaning as Fig. 1.

In Fig. 2 the quenched G_M^* data is very well described by our model [which is also stated in Table II in the column $\chi^2(G_M^*)$]. The exception is the case for the lightest pion mass $m_\pi = 411$ MeV, where pion cloud effects may start

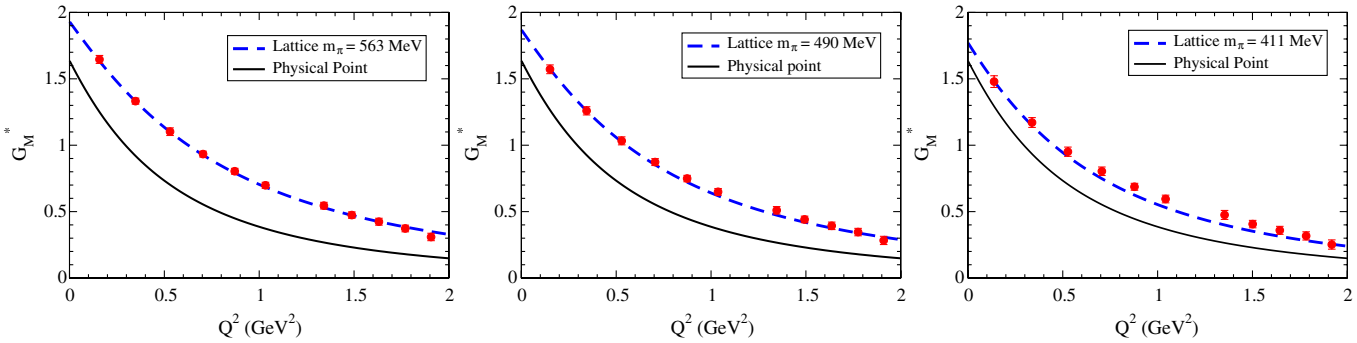

FIG. 2 (color online). Magnetic dipole form factor G_M^* in quenched QCD [10]. The valence quark contribution at the physical point (solid line) is included as reference.

TABLE III. D-state parameters of the Δ wave function as result of the fit to the quenched lattice data [10]. The coefficient $\lambda_{D1} = 1.0319$, in Eq. (11) is determined by the values of α_3 and α_4.

α_2	α_3, α_4	a, b
0.3421	0.3507	0.0856
	0.3377	0.0857

to be important [37] but are absent in the valence quark model.

The model describes fairly well the lattice data for the quadrupole form factors. The quality decreases for the lightest pion mass, which is due to the omission of explicit pion cloud effects in our approach. It is encouraging that the χ^2 values are lower than the ones found for the fit in the physical region [13], indicating that the procedure used here is more natural. Still, it should be said that the χ^2's obtained also possibly reflect the still poorer quadrupole lattice statistics and the narrower range of the lattice data, when compared to the experimental data or even to the lattice data for G_M^*.

A study of the dependence of the $\gamma N \to \Delta$ form factors on the pion mass and Q^2 was also considered in Refs. [26,27]. The lattice QCD data for G_M^* in Refs. [9,26], manifests a significant difference from the more recent analysis of Ref. [10]. For a similar pion mass, the results of Ref. [9] are larger than the ones presented in Ref. [10].

V. QUADRUPOLE FORM FACTORS AT THE PHYSICAL POINT

After the parametrization of the D states was obtained from the lattice data, we can now apply it to the physical region. This requires us to use the experimental data, in the form of the two ratios

$$R_{EM} = -\frac{G_E^*(Q^2)}{G_M^*(Q^2)}, \qquad R_{EM} = -\frac{|\mathbf{q}|}{2m_\Delta}\frac{G_C^*(Q^2)}{G_M^*(Q^2)}, \quad (14)$$

where $|\mathbf{q}|$ is the photon momentum in the Δ rest frame, and we use the empirical parametrization of Ref. [27]:

$$G_M^*(Q^2) = 3G_D \exp(-0.21Q^2)\sqrt{1 + \frac{Q^2}{(m_N + m_\Delta)^2}}. \quad (15)$$

In the last expression $G_D = (1 + Q^2/0.71)^{-2}$ represents the dipole form factor. The quality of the parametrization was studied in Ref. [13].

Since D states extracted from the lattice data and applied to the physical region include only the contribution of the valence quarks, they necessarily underestimate the experimental data. To fill the gap between the valence contribution and the experimental data, we have to consider contributions from the pion cloud. In particular we consider the pion cloud parametrization used in Ref. [13], where the pion cloud contributions to G_E^* and G_C^* were determined using large-N_c relations [40,41] between those form factors and G_{En} (the neutron electric form factor):

$$G_E^\pi(Q^2) = \left(\frac{m_N}{m_\Delta}\right)^{3/2}\frac{m_\Delta^2 - m_N^2}{2\sqrt{2}}\frac{G_{En}(Q^2)}{Q^2}, \quad (16)$$

$$G_C^\pi(Q^2) = \sqrt{\frac{2m_N}{m_\Delta}}m_N m_\Delta \frac{G_{En}(Q^2)}{Q^2}. \quad (17)$$

To evaluate G_{En}, we took model II of [32] for the nucleon. The results are presented in Fig. 4. In that figure we compare the final results for G_E^* and G_C^* and include the lattice data to show the magnitude of the valence contributions. The valence contributions are also compared with the parametrization of the valence contribution from the Sato and Lee model [31]. Note that the Sato and Lee parametrization gives a contribution similar to our model for $Q^2 > 0.5$ GeV^2, for both G_E^* and G_C^*. It lies above our results, overpredicting the lattice data, for lower Q^2.

In conclusion, by fixing the D-state components by the lattice data and considering a pion cloud parametrization, derived from the large-N_c limit at the physical point, we obtained a fairly good description of the quadrupole lattice data, in the range $Q^2 < 1.5$ GeV^2. The exception is the region $Q^2 < 0.2$ GeV^2, where a small $D1$ mixture, when compared with Ref. [13], underpredicts the G_C^* data. Note, however, that there is some discrepancy between different experimental data in that region [13]. The planned data from the CLAS collaboration for that range would be important to clarify the low Q^2 behavior of G_C^* [31,42].

A complete lattice QCD data set is available in Ref. [10]. It presents lattice data in the quenched approximation and the unquenched data based on Wilson and also on a hybrid action. In this work, we restrict our application to the quenched data. There are three main reasons for this restriction:

(i) There is a significant discrepancy between the quenched and unquenched data, particularly for the results of G_M^* with heavier masses. In this regime we would expect small pion cloud effects, implying negligible differences between quenched and unquenched results. In Fig. 5 we compare the lattice data corresponding to $m_\pi = 563$ MeV (quenched) and $m_\pi = 594$ MeV (hybrid action). There is a significant difference between those two data sets, with the Wilson data associated with $m_\pi = 691$ MeV being more consistent with the hybrid action ($m_\pi = 563$ MeV).

(ii) There are differences between the two unquenched results, in particular, for the value of m_ρ. The extension of our model depends on the (quenched) ρ mass. It is not clear whether the extension of our model is

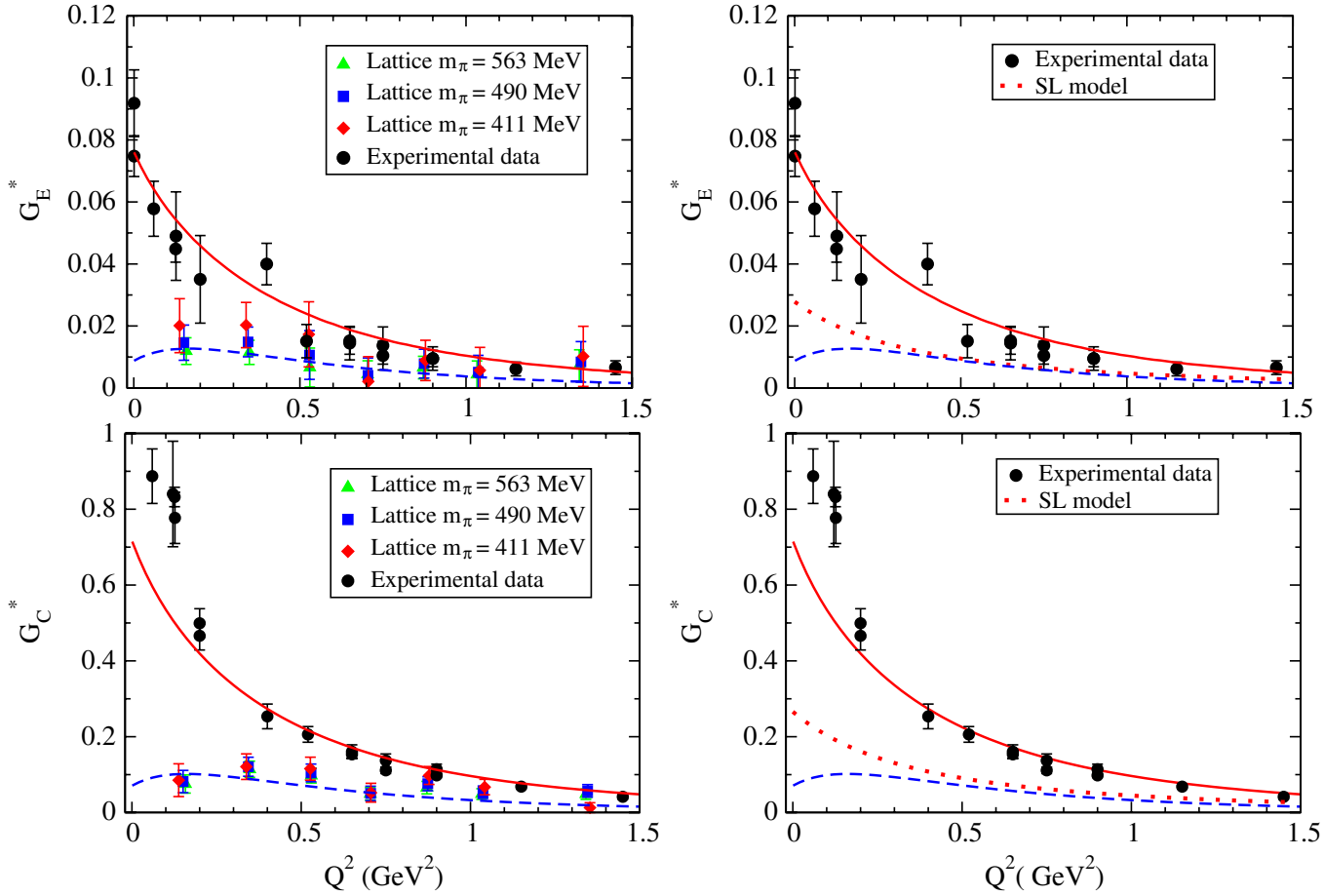

FIG. 4 (color online). Extension to the physical region using the quenched parametrization. The dashed line represents the valence contribution. The solid line represents the combination of valence and pion cloud effects. Physical data from Jlab [1,2], MAMI [3], LEGS , and MIT-Bates [5]. Quenched lattice QCD data from [10]. Sato and Lee parametrization from [31].

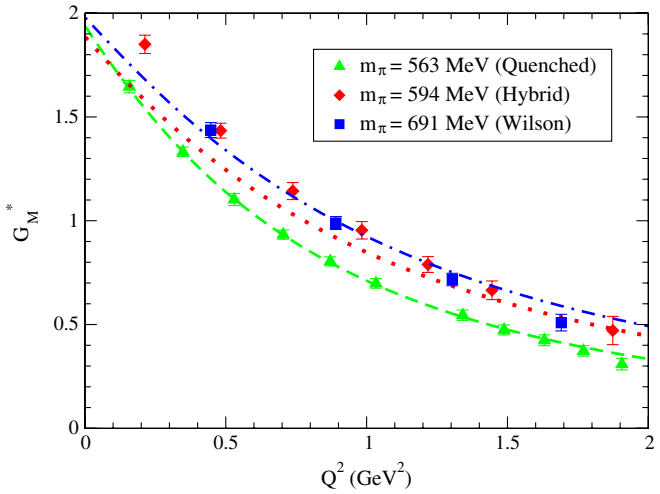

FIG. 5 (color online). Dependence of G_M^* with m_π, for quenched ($m_\pi = 563$ MeV), Wilson ($m_\pi = 691$ MeV), and Hybrid ($m_\pi = 594$ MeV). The lines correspond to the result of the VMD model with m_N, m_ρ, and m_Δ associated with the quenched data for $m_\pi = 563$ MeV (dashed line), Wilson action: $m_\pi = 594$ MeV (dotted line), and Hybrid action: $m_\pi = 691$ MeV (dash-dotted line).

justified for the unquenched calculations, where the nucleon, Δ, and ρ masses would differ from the quenched masses. We would expect only minor differences for heavier pion masses (say $m_\pi > 480$ MeV). However, the significant difference between the ρ mass for the Wilson action data with $m_\pi = 509$ MeV ($m_\rho = 887$ MeV) and the hybrid action with $m_\pi = 490$ MeV ($m_\rho = 949$ MeV) is difficult to explain.

(iii) Finally, there is only a limited number of unquenched quadrupole data points for large pion masses. Since the unquenched lattice data for light pion masses as 353 MeV (hybrid action) and 384 MeV (Wilson action) are expected to be contaminated with pion cloud effects, which cannot be simulated by our valence quark model, those points would have to be excluded. We would then be left with 6 or 8–9 quadrupole points, respectively, for the Wilson and hybrid action (to be compared with 21 from quenched data), and with such a small number of constraints the fit would naturally become meaningless.

Apart from the disagreement observed in the description of the magnetic dipole form factor, the Wilson and hybrid action lattice data suggest a weaker falloff of the electric quadrupole form factor G_E^* when compared to the quenched prediction. This result is also observed for the physical point extrapolation.

Once the differences between the two unquenched results are understood, and the disagreement between quenched and unquenched results for $m_\pi \sim 600$ MeV is clarified, it would be interesting to use also unquenched data to extract the contribution of the D states, using the procedure suggested here. The increase of statistics in both quenched and unquenched lattice data could also help to constrain the effects of the Δ D states in the $\gamma N \to \Delta$ transition.

VI. CONCLUSIONS

In this work we study the valence quark contributions to the $\gamma N \to \Delta$ transition in the lattice QCD regime, in the framework of the covariant spectator formalism. The nucleon and the Δ wave functions are not derived from a wave equation but are parametrized in terms of the nucleon and Δ symmetry structure for spin, isospin, and angular momentum. By construction, the formalism includes only valence quark degrees of freedom, whereas meson cloud mechanisms are not taken into account.

As discussed extensively in the literature (see Refs. [13,26]), valence contributions do not dominate the quadrupole form factors at the physical point, where the pion cloud effects dominate instead, while the opposite happens in the lattice QCD regime. In an attempt to explain the significant difference between the experimental data and the emerging simulations of lattice QCD with a decreasing pion mass, but still small chiral effects associated with the light pions, we started by comparing our quark model directly to the lattice data. In contrast to the dominant contribution controlled by the nucleon and Δ S states, the Δ D states, being a second order correction, are more sensitive to the lattice data. This sensitivity provides a clean evaluation of the valence quark contribution, since in the physical region the valence quark contribution is masked by the overwhelmingly larger contribution of the pion cloud, and consequently the D-state parametrization cannot be accurately constrained.

Accordingly, we found that by fixing the D states by the physical data first does not lead to a good description of the lattice QCD data. We also verified that, inversely, when the D states are first fixed in the lattice QCD regime, then a good description of the physical data is possible. In fact, adding the valence quark contribution extrapolated from quenched lattice QCD to the physical mass regime, with an estimate of the pion cloud based on the large-N_c limit [13,40], the experimental data for the $\gamma N \to \Delta$ quadrupole form factor is well described. An even more accurate description of the experimental data can, in principle, be obtained by considering more and more precise lattice QCD data and a more sophisticated estimate of the pion cloud.

The fit to the lattice QCD data varied five parameters associated with the valence D-states. The result of the fit suggests an identical admixture of the $D1$ and $D3$ states.

We conclude that lattice QCD data are important to constrain valence quark models. Since lattice calculations with $m_\pi > 400$ MeV valence quark effects dominate over the pion cloud, lattice data can be used to study and separate those effects.

ACKNOWLEDGMENTS

G. R. wants to thank Jozef Dudek, Kostas Orginos, and Franz Gross for the helpful discussions. The authors thank Constantia Alexandrou for sharing details of the lattice data presented in Ref. [10] and Alfred Stadler for the review of the final text. This work was partially supported by Jefferson Science Associates, LLC under U.S. DOE Contract No. DE-AC05-06OR23177. G. R. was supported by the Portuguese Fundação para a Ciência e Tecnologia under Grant No. SFRH/BPD/26886/2006. This work has been supported in part by the European Union (HadronPhysics2 project ''Study of strongly interacting matter'').

[1] V. V. Frolov *et al.*, Phys. Rev. Lett. **82**, 45 (1999); K. Joo *et al.* (CLAS Collaboration), Phys. Rev. Lett. **88**, 122001 (2002).
[2] M. Ungaro *et al.* (CLAS Collaboration), Phys. Rev. Lett. **97**, 112003 (2006).
[3] R. Beck *et al.*, Phys. Rev. C **61**, 035204 (2000); T. Pospischil *et al.*, Phys. Rev. Lett. **86**, 2959 (2001); D. Elsner *et al.*, Eur. Phys. J. A **27**, 91 (2006); N. F. Sparveris *et al.*, Phys. Lett. B **651**, 102 (2007); S. Stave *et al.*, Eur. Phys. J. A **30**, 471 (2006).
[4] G. Blanpied *et al.*, Phys. Rev. C **64**, 025203 (2001); Phys. Rev. Lett. **79**, 4337 (1997).
[5] C. Mertz *et al.*, Phys. Rev. Lett. **86**, 2963 (2001); N. F. Sparveris *et al.* (OOPS Collaboration), Phys. Rev. Lett. **94**, 022003 (2005).
[6] C. Alexandrou *et al.*, Phys. Rev. D **79**, 014507 (2009); Nucl. Phys. **A825**, 115 (2009).
[7] C. Aubin, K. Orginos, V. Pascalutsa, and M. Vanderhaeghen, Phys. Rev. D **79**, 051502(R) (2009).
[8] D. B. Leinweber, T. Draper, and R. M. Woloshyn, Phys. Rev. D **48**, 2230 (1993).
[9] C. Alexandrou, Ph. de Forcrand, H. Neff, J. W. Negele, W.

Schroers, and A. Tsapalis, Phys. Rev. Lett. **94**, 021601 (2005); C. Alexandrou *et al.*, Phys. Rev. D **69**, 114506 (2004).
[10] C. Alexandrou, G. Koutsou, H. Neff, J. W. Negele, W. Schroers, and A. Tsapalis, Phys. Rev. D **77**, 085012 (2008).
[11] H. F. Jones and M. D. Scadron, Ann. Phys. (N.Y.) **81**, 1 (1973).
[12] G. Ramalho, M. T. Peña, and F. Gross, Eur. Phys. J. A **36**, 329 (2008).
[13] G. Ramalho, M. T. Peña, and F. Gross, Phys. Rev. D **78**, 114017 (2008).
[14] C. Becchi and G. Morpurgo, Phys. Lett. **17**, 352 (1965).
[15] N. Isgur, G. Karl, and R. Koniuk, Phys. Rev. D **25**, 2394 (1982).
[16] M. M. Giannini, L. Tiator, D. Drechsel, S. Kamalov, M. M. Giannini, E. Santopinto, and A. Vassallo, Eur. Phys. J. A **19**, 55 (2004); M. Aiello, M. Ferraris, M. M. Giannini, M. Pizzo, and E. Santopinto, Phys. Lett. B **387**, 215 (1996).
[17] S. Capstick and B. D. Keister, Phys. Rev. D **51**, 3598 (1995).
[18] B. Julia-Diaz and D. O. Riska, Nucl. Phys. **A757**, 441 (2005).
[19] M. De Sanctis, M. M. Giannini, E. Santopinto, and A. Vassallo, Eur. Phys. J. A **19**, 81 (2004).
[20] V. M. Braun, A. Lenz, and M. Wittmann, Phys. Rev. D **73**, 094019 (2006).
[21] V. Pascalutsa, M. Vanderhaeghen, and S. N. Yang, Phys. Rep. **437**, 125 (2007).
[22] A. Faessler, T. Gutsche, B. R. Holstein, V. E. Lyubovitskij, D. Nicmorus, and K. Pumsa-ard, Phys. Rev. D **74**, 074010 (2006).
[23] D. H. Lu, A. W. Thomas, and A. G. Williams, Phys. Rev. C **55**, 3108 (1997).
[24] A. J. Buchmann, E. Hernandez, and A. Faessler, Phys. Rev. C **55**, 448 (1997); A. J. Buchmann, E. Hernandez, U. Meyer, and A. Faessler, Phys. Rev. C **58**, 2478 (1998); U. Meyer, E. Hernandez, and A. J. Buchmann, Phys. Rev. C **64**, 035203 (2001).
[25] Q. B. Li and D. O. Riska, Nucl. Phys. **A766**, 172 (2006); Phys. Rev. C **73**, 035201 (2006).
[26] V. Pascalutsa and M. Vanderhaeghen, Phys. Rev. D **73**, 034003 (2006); Phys. Lett. B **636**, 31 (2006).
[27] T. A. Gail and T. R. Hemmert, Eur. Phys. J. A **28**, 91 (2006).
[28] D. Arndt and B. C. Tiburzi, Phys. Rev. D **69**, 014501 (2004).
[29] T. Sato and T. S. H. Lee, Phys. Rev. C **63**, 055201 (2001); G. L. Caia, L. E. Wright, and V. Pascalutsa, Phys. Rev. C **72**, 035203 (2005).
[30] D. Drechsel, S. S. Kamalov, and L. Tiator, Eur. Phys. J. A **34**, 69 (2007); S. S. Kamalov, S. N. Yang, D. Drechsel, O. Hanstein, and L. Tiator, Phys. Rev. C **64**, 032201(R) (2001); D. Drechsel, O. Hanstein, S. S. Kamalov, and L. Tiator, Nucl. Phys. **A645**, 145 (1999).
[31] B. Julia-Diaz, T. S. H. Lee, T. Sato, and L. C. Smith, Phys. Rev. C **75**, 015205 (2007).
[32] F. Gross, G. Ramalho, and M. T. Peña, Phys. Rev. C **77**, 015202 (2008).
[33] F. Gross, G. Ramalho, and M. T. Peña, Phys. Rev. C **77**, 035203 (2008).
[34] G. Ramalho and M. T. Peña, J. Phys. G **36**, 085004 (2009).
[35] M. Gockeler, T. R. Hemmert, R. Horsley, D. Pleiter, P. E. L. Rakow, A. Schafer, and G. Schierholz (QCDSF Collaboration), Phys. Rev. D **71**, 034508 (2005).
[36] G. Ramalho and M. T. Peña, arXiv:0812.0187.
[37] W. Detmold, D. B. Leinweber, W. Melnitchouk, A. W. Thomas, and S. V. Wright, Pramana **57**, 251 (2001); J. D. Ashley, D. B. Leinweber, A. W. Thomas, and R. D. Young, Eur. Phys. J. A **19**, 9 (2004).
[38] F. Gross, Phys. Rev. **186**, 1448 (1969); F. Gross, J. W. Van Orden, and K. Holinde, Phys. Rev. C **45**, 2094 (1992).
[39] F. Gross and P. Agbakpe, Phys. Rev. C **73**, 015203 (2006).
[40] V. Pascalutsa and M. Vanderhaeghen, Phys. Rev. D **76**, 111501(R) (2007).
[41] A. J. Buchmann and E. M. Henley, Phys. Rev. C **63**, 015202 (2000); Phys. Rev. D **65**, 073017 (2002).
[42] S. Stave *et al.* (A1 Collaboration), Phys. Rev. C **78**, 025209 (2008).